Structure and Anti-TB Activity of Trachylobanes from the Liverwort *Jungermannia exsertifolia ssp. cordifolia*

Jochen M. Scher,*[,†,§] Andreas Schinkovitz,[‡,§] Josef Zapp,[†] Yuehong Wang,[‡] Scott G. Franzblau,[‡] Hans Becker,[†] David C. Lankin,[‡] and Guido F. Pauli[‡]

Pharmakognosie und Analytische Phytochemie, Universität des Saarlandes, Gebäude 32, D-66041 Saarbrücken, Germany, and Institute for Tuberculosis Research, Department of Medicinal Chemistry and Pharmacognosy, and PCRPS, College of Pharmacy, University of Illinois at Chicago, Chicago, Illinois 60612

Received December 20, 2009

In the critical search for new antituberculosis lead compounds, bryophytes represent a largely untapped resource of chemically diverse structures. From the liverwort *Jungermannia exsertifolia* subsp. *cordifolia*, 11 new trachylobane diterpene derivatives, as well as three known compounds, were isolated. Their structures were elucidated by spectroscopic means, and full ^{1}H NMR spin analysis of one model compound confirmed the relative configurational assignments of the congeners. Four of the isolates exhibited noticeable activity against virulent *Mycobacterium tuberculosis* $H_{37}Rv$ with minimal inhibitory concentrations of 61−24 μg/mL. This finding suggests that bryophytes in general and trachylobanes in particular deserve further attention in the search for new antimycobacterial leads.

Responsible for about 9.2 million new infections and an estimated 1.8 million casualties every year, tuberculosis (TB) represents one of the most menacing diseases to mankind.[1] An estimated one-third of the world's population is latently infected with *Mycobacterium tuberculosis*, and the pathogen is known to commonly cause co-infection among HIV-positive or immune-impaired individuals. Furthermore, multi-drug-resistant (MDR) as well as extensively drug-resistant (EDR) strains of *M. tuberculosis* aggravate the global TB situation. Considering that no new anti-TB drugs have been developed in decades, new antimycobacterial lead compounds are urgently needed.

Many plants have been tested for their antimycobacterial effects and have yielded, through isolation, several compounds that exhibit promising activities.[2−4] However, only a few studies have been performed in order to evaluate the antimycobacterial activities of bryophytes.[5,6] In the present study, we describe a comprehensive phytochemical and biological evaluation of the liverwort *Jungermannia exsertifolia* subsp. *cordifolia* with special focus on antimycobacterial activities against *M. tuberculosis* $H_{37}Rv$. The following describes (i) an isolation strategy for 14 trachylobane diterpenes from *J. exsertifolia* subsp. *cordifolia*, (ii) their activity profile against *M. tuberculosis* $H_{37}Rv$, (iii) their structure elucidation based on extensive NMR, GC-MS, IR, and HRES MS analyses, and (iv) a full ^{1}H NMR spin analysis of one model compound with the goal of confirming NMR structural assignments for the class of trachylobanes.

Results and Discussion

The unique structural features of the trachylobane diterpenes is represented by a pentacyclic carbon skeleton with a tricyclo[3.2.1.0]octane system incorporated into ring C.[7] Compounds of this kind were first isolated from the resin of *Trachylobium verrucosum* (Leguminosae).[8] The first trachylobane diterpene obtained from the botanical class of Hepaticae was isolated from the liverwort *J. exsertifolia* subsp. *cordifolia* and identified as 3α,18-dihydroxytrachyloban-19-oic acid.[9] All trachylobanes isolated so far belong to the *enantio* series (α-substituents are located above and β-substituents below the plane of the molecule).[10]

Trachylobane diterpenes (see ref 10 for a review) have been associated with various pharmacological properties such as the inhibition of larval development,[11] antifeedant and toxic effects,[12] and apoptosis-inducing activities in human promyelocytic leukemia cells.[13] Trachylobanes have been reported to exhibit antimicrobial activities against *Staphylococcus aureus* and *Mycobacterium smegmatis*,[5,14] and an initial phytochemical study of *J. exsertifolia* trachylobanes has previously been reported.[15] However, their antimycobacterial activity against virulent *M. tuberculosis* has not previously been explored.

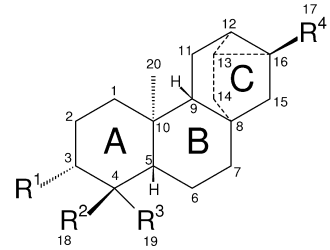

	R^1	R^2	R^3	R^4
	C-3β	C-4α	C-4β	C-16α
1	-OH	$-CH_3$	$-CH_3$	$-CH_3$
2	=O	$-CH_3$	$-CH_3$	$-CH_3$
3	$-OCOCH_3$	$-CH_3$	$-CH_3$	$-CH_3$
4	$-OCOCH_3$	$-CH_2OH$	$-CH_3$	$-CH_3$
5	-OH	$-CH_2OCOCH_3$	$-CH_3$	$-CH_3$
6	$-OCOCH_3$	$-CH_3$	$-CH_2OH$	$-CH_3$
7	$-OCOCH_3$	-CHO	$-CH_3$	$-CH_3$
8	$-OCOCH_3$	$-CH_3$	-CHO	$-CH_3$
9	$-OCOCH_3$	$-CH_3$	$-CH_3$	$-CH_2OH$
10	-H	$-CH_3$	$-CH_3$	$-CH_2OH$
11	-H	$-CH_3$	$-CH_3$	-CHO
12	$-OCOCH_3$	$-CH_2OCOCH_3$	-COOH	$-CH_3$
13	-OH	$-CH_2OH$	$-CH_3$	$-CH_3$
14	-OH	$-CH_3$	$-CH_3$	-COOH

From a CH_2Cl_2 extract of *J. exsertifolia*, 11 new diterpenes, *ent*-3β-acetoxy-18-hydroxytrachylobane (**4**), *ent*-18α-acetoxy-3β-hydroxytrachylobane (**5**), *ent*-3β-acetoxy-19-hydroxytrachylobane (**6**), *ent*-3β-acetoxytrachyloban-18-al (**7**), *ent*-3β-acetoxytrachyloban-19-al (**8**), *ent*-3β-acetoxy-17-hydroxytrachylobane (**9**), *ent*-17-hydroxytrachylobane (**10**), *ent*-trachyloban-17-al (**11**), *ent*-3β,18α-diacetoxy-19-trachylobanoic acid (**12**), *ent*-3β,18α-dihydroxytrachylobane (**13**), and *ent*-3β-hydroxy-17-trachylobanoic acid (**14**), were isolated by using a combination of vacuum liquid chromatography (VLC), size exclusion chromatography

* To whom correspondence should be addressed. Tel: +49 7351-168609. Fax: +49 7351-54 5132. E-mail: jochen.scher@web.de.
† Universität des Saarlandes.
§ Equal contributors.
‡ University of Illinois at Chicago.

10.1021/np900806j
Published on Web 03/30/2010

Table 1. ^{13}C NMR Data of the Trachylobanes **1**−**14**

position	1	2	3	4	5	6	7	8	9	10	11	12	13	14
1	37.46	38.04	37.13	37.02	37.21	37.12	36.80[a]	36.46	37.06	39.16	39.04	37.04	37.13	37.29
2	26.93	34.08	23.28	23.16	25.78	23.26	22.25	23.62	23.22	18.16	18.06	23.17	26.57	26.92
3	79.16	217.38	81.08	74.86	72.66	83.13	73.51	78.64	80.98	42.12	42.03	73.00	77.10	78.98
4	38.69	47.62	37.95	42.30	41.95	42.31	54.27	51.81[a]	37.62	33.01	33.02	51.72	41.81	38.25
5	55.14	55.55	55.25	46.52	48.00	55.95	47.65	57.05	55.17	56.12	55.94	49.25	49.68	54.91
6	19.91	21.12	19.82	19.23	19.73	20.37	21.91	20.18	19.78	20.15	20.00	21.22[a]	20.07[a]	19.76
7	38.91	38.32	38.80	38.30	38.59	38.97	37.98	38.51	38.66	38.93	38.36	38.41	38.59	38.69
8	40.51	40.46	40.53	40.46	40.48	40.47	40.68	40.23	40.33	40.60	40.11	40.31	40.49	40.02
9	53.14	52.43	53.06	52.86	53.15	53.01	52.94	51.79[a]	52.94	53.22	52.45	52.76	53.13	52.08
10	38.04	37.76	37.64	37.65	37.90	37.69	36.77[a]	37.85	37.98	38.38	38.45	38.24	37.88	37.29
11	19.68	19.65	19.70	19.71	19.68	19.96	19.65	20.18[a]	19.58	19.62	19.14	19.82[a]	19.70[a]	19.31
12	20.57	20.46	21.29	20.52	20.52	20.47	20.33	20.32	18.83	18.98	30.29	20.32	20.51	31.71
13	24.24	24.20	24.23	24.19	24.19	24.13	24.14	24.11	22.07	22.19	24.59	22.40	24.22	25.54
14	33.40	33.25	33.43	33.44	33.34	33.23	33.35	33.17	32.97	33.07	32.06	33.02	33.40	32.36
15	50.38	50.21	50.36	50.22	50.23	50.12	50.17	50.18	45.62	45.85	40.78	49.94	50.33	42.70
16	22.49	22.50	22.52	22.52	22.47	22.48	22.52	22.51	29.67	29.90	41.88	22.40	22.49	40.03
17	20.55	20.46	20.56	20.52	20.52	20.21	20.43	20.43	67.73	67.93	201.08	20.36	20.50	180.83
18	28.07	26.09	28.05	64.43	67.12	22.13	204.44	20.78	16.59	21.67	21.59	62.53	72.05	28.00
19	15.47	21.55	16.61	12.75	11.93	63.95	9.36	204.63	28.02	33.39	33.30	176.93	11.25	15.41
20	14.64	14.10	14.71	15.25	15.19	15.05	14.89	15.27	14.75	14.62	14.77	12.68	14.97	14.80
21			170.93	172.31	171.61	169.48	170.28	170.48				170.69		
22			20.52	21.18	20.52	21.40	21.00	21.10				21.15		
23												170.49		
24												20.74		

[a] Signals within a column are interchangeable.

(SEC), and preparative HPLC. In addition, three known compounds were isolated and identified as *ent*-3β-hydroxytrachylobane (**1**), *ent*-trachyloban-3-one (**2**),[16] and *ent*-3β-acetoxytrachylobane (**3**).[17]

Compound **4** was obtained as a white solid. Its molecular formula was established as $C_{22}H_{34}O_3$ through EIHRMS ($[M]^+$: 346.2523). Strong bands in the IR spectrum at 1717 cm^{-1} (C═O), 1269 and 1055 cm^{-1} (C−O) indicated the presence of a carbonyl group. This was confirmed by a signal observed in the ^{13}C NMR spectrum at δ_C 172.31 (Table 1). Additionally, the presence of a primary alcohol moiety located at C-18 was confirmed by the ^{13}C chemical shift (δ_C 64.43) of this particular carbon. Furthermore, analysis of the ^{13}C NMR data revealed the presence of a secondary alcohol group at C-3 (δ_C 74.86), but no other functionalities. The observed 22 carbon signals were assigned to five non-proton-binding carbons (four quaternary and one carbonyl carbon), five methine, eight methylene, and four methyl carbons by HMBC and DEPT experiments. The ^1H NMR spectrum (Table 2) showed the presence of four methyl singlets at δ_H 0.63, 0.97, 1.10, and 2.05. The latter is very specific for an acetoxy methyl group. Two characteristic ^1H signals observed at δ_H 0.55 (td, J = 7.8, 2.5 Hz) and at 0.79 (dd, J = 7.8, 3.1 Hz) indicated the presence of a cyclopropane ring. consistent with the structure of the trachylobane diterpenes. ^1H and ^{13}C NMR data of **4** exhibited general features similar to those observed for *ent*-3β-acetoxytrachylobane **3**.[17] The main difference in the ^1H NMR spectra between **4** and **3** was the replacement of the methyl singlet H-18 at δ_H 0.82 by two oxymethylene protons (H-18a, δ_H 2.86, d, and H-18b, δ_H 3.26, d, ^2J = 12.5 Hz; C-18, δ_C 64.43).

The HMBC spectrum of **4** displayed a strong long-range coupling between the carbonyl carbon at δ_C 172.31 and the oxymethine proton H-3 at δ_H 4.83 (dd, J = 12.1, 4.4 Hz) and a methyl group, which proved that the oxygen at C-3 was acetylated. According to nomenclature conventions, in the *ent* series of trachylobane derivatives α-substituents are located above and β-substituents below the plane of the molecule.[10,24] The results of NOESY experiments exhibited strong correlation cross-peaks between H-5 and H-3 as well as between the methyl groups at C-19 and C-20. These observations indicated that the methyl groups at C-19 and C-20 and the acetylated hydroxy group at C-3 are β-oriented, whereas the bridgehead H-5 as well as H-3 are α-oriented. The A/B ring junction was therefore assigned to be *trans*. Thus, the structure of **4** was established as *ent*-3β-acetoxy-18-hydroxytrachylobane.

Compound **5**, by virtue of its isomeric nature, shared common spectroscopic features with **4**. Its molecular formula, $C_{22}H_{34}O_3$, was determined by EIHRMS (*m*/*z* 346.2508 $[M]^+$). Infrared absorptions at 2926 and 1744 cm^{-1} provided evidence for hydroxy and carbonyl groups, respectively. The presence of a cyclopropane ring was indicated from the ^1H NMR data, which exhibited two specific high-field signals at δ_H 0.56 (H-12, td, J = 7.8, 2.3 Hz) and δ_H 0.81 (H-13, dd, J = 7.8, 3.3 Hz). This assignment is in accordance with ^{13}C shifts observed for their corresponding carbons at δ_C 20.52 (C-12), 24.19 (C-13), and 22.47 (C-16, quaternary). Moreover, the carbonyl signal at δ_C 171.61 indicated an esterified carboxyl group, which showed an HMBC correlation to both an oxymethylene group (C-18) and a acetoxy methyl function, providing evidence for an acetylated hydroxymethylene substituent. The secondary alcohol group at C-3 was identified from a signal appearing at δ_H 3.36 (H-3, dd, J = 9.0, 7.0 Hz) together with its corresponding carbon signal at δ_C 72.66. C-3 further showed HMBC correlations to three protons at δ_H 0.74 (H-19, s), 1.58 (H-2eq or H-2ax), and 1.52 dt (H-1eq, dt J = 13.2, 3.5). Strong NOESY correlation cross-peaks were observed between H-3 and the oxymethylene group as well as between H-5 and H-3, suggesting they are α-oriented. On the basis of these considerations, the C-19 methyl group attached to C-4 was assigned to be in a β-orientation. Additional NOESY interactions were observed between the C-20 methyl group at C-10 and the C-19 methyl group at C-4, which supported the assignment of β-orientation for the latter. From both direct observations and by comparing the NMR data from structurally related compounds (e.g., **1**, **2**, and **4**), the structure of **5** was identified as *ent*-18α-acetoxy-3β-hydroxytrachylobane.

The ^1H and ^{13}C NMR data of **6** were similar to those of **4**. Its molecular formula was established as $C_{22}H_{34}O_3$ (*m*/*z* 346.2508 $[M]^+$) through EIHRMS, making **6** isomeric with **4**. The ^{13}C NMR and ^1H NMR spectra revealed the presence of two hydroxy groups, of which one was acetylated. Strong NOESY correlation cross-peaks were observed between H-5 (δ_H 0.91, dd, J = 12.1, 1.7 Hz) and H-3 (δ_H 4.58, dd, J = 10.4, 5.9 Hz) as well as between the protons of the C-18 methyl group and H-3. These findings indicated the placement of both the hydroxylated methylene group C-19 and the acetylated secondary hydroxy group attached to C-3 in a β-orientation, suggesting that *ent*-3β-acetoxy-19-hydroxytrachylobane is consistent with structure **6**. The latter represents a diastereomer of **4**.

Table 2. ^{1}H NMR Data of the Trachylobanes **2**−**14**

	δ_C [ppm], multiplicity (J [Hz])[a]						
pos	**2**	**3**	**4**	**5**	**6**	**7**	**8**
1ax	1.24 m	0.92 m	0.90 dt (13.7, 3.7)	0.83 m	0.94 m	1.02 m	1.01 m
1eq	1.71 ddd (14.5, 7.2, 2.4)	1.51 td (13.4, 3.7)	1.54 m	1.52 dt (13.2, 3.5)	1.54 m	1.61 td (13.6, 3.5)	1.65 m
2ax	2.28 ddd (15.9, 6.0, 3.2)	1.58 m	1.52 m	1.58 m	1.68 m	1.70 m	1.88 brd
2eq	2.54 ddd (15.9, 12.3, 7.0)	1.57 m	1.77 dq (15.9, 13.5, 4.1)	1.58 m	1.68 m	1.70 m	1.96 m
3ax		4.44 dd (10.4, 5.9)	4.83 dd (12.1, 4.4)	3.36 dd (9.0, 7.0)	4.58 dd (10.4, 5.9)	4.91 dd (11.3, 5.1)	4.62 dd (12.0, 5.3)
5ax	1.20 m	0.79 m	1.31 brdd (11.7, 1.1)	0.96 m	0.91 dd (12.1, 1.7)	1.31 m	1.06 m
6ax	1.42 m	1.29 dd (12.1, 3.5)	1.24 m	1.31 m	1.28 m	1.65 m	1.26 m
6eq	1.41 m	1.45 m	1.46 m	1.38 m	1.28 m	1.70 m	1.68 m
7ax	1.44 m	1.39 m	1.40 m	1.37 m	1.31 m	1.36 m	1.45 td (13.4, 3.0)
7eq	1.37 m	1.35 m	1.46 m	1.30 m	1.42 m	1.36 m	1.32 dt (13.4, 4.0)
9ax	1.15 m	1.06 ddd (11.0, 7.4, 1.2)	1.15 m	1.08 m	1.07 ddd (11.3, 7.1, 1.1)	1.04 s	1.04 s
11a=α	1.92 ddd (14.6, 11.3, 3.2)	1.85 ddd (14.4, 11.4, 3.1)	1.86 ddd (14.4, 11.3, 3.1)	1.86 ddd (14.5, 11.3, 3.1)	1.88 ddd (14.6, 11.3, 3.0)	1.89 ddd (14.5, 11.3, 3.1)	1.89 m
11b=β	1.71 ddd (14.6, 7.1, 2.4)	1.63 ddd (14.6, 7.2, 2.3)	1.63 ddd (14.5, 7.1, 2.2)	1.65 ddd (14.5, 7.1, 2.5)	1.61 ddd (14.4, 7.2, 2.2)	1.61 td (13.8, 3.6)	1.62 ddd (14.5, 7.2, 2.3)
12	0.59 td (7.5, 2.7)	0.55 td (7.8, 2.6)	0.55 td (7.8, 2.5)	0.56 td (7.8, 2.3)	0.55 td (7.9, 2.5)	0.58 td (7.8, 2.5)	0.57 td (7.8, 2.5)
13	0.84 dd (7.8, 3.2)	0.80 m	0.79 dd (7.8, 3.1)	0.81 dd (7.8, 3.3)	0.80 dd (7.8, 3.1)	0.82 dd (8.0, 3.2)	0.80 dd (7.8, 3.1)
14a	2.06 d (11.8)	2.03 d (11.7)	2.01 d (12.0)	2.02 d (11.8)	1.98 d (12.0)	2.01 d (11.7)	1.94 d (11.7)
14b	1.20 ddd (11.8, 3.2, 1.7)	1.14 ddd (11.9, 3.2, 1.7)	1.13 m	1.14 ddd (12.0, 2.9 1.5)	1.14 ddd (11.9, 3.2, 1.7)	1.14 m	1.14 m
15a=β	1.40 m	1.37 d (11.3)	1.39 d (6.8)	1.38 d (10.8)	1.37 d (11.3)	1.37 m	1.40 d (11.3)
15b=α	1.21 d (11.1)	1.22 d (11.3)	1.23 d (11.0)	1.23 d (11.0)	1.21 d (11.3)	1.26 d (11.4)	1.21 d (11.2)
17	3H 1.13 s	3H 1.11 s	3H 1.10 s	3H 1.11 s	3H 1.11 s	3H 1.12 s	3H 1.11 s
18	3H 1.04 s	3H 0.82 s	2.86 d (12.5) 3.26 d (12.5)	3.74 d (11.5) 4.17 d (11.5)	3H 1.03 s	9.22 s	3H 1.04 s
19	3H 1.00 s	3H 0.82 s	3H 0.63 s	3H 0.74 s	3.34 d (11.3) 4.11 d (11.8)	3H 1.03 s	10.00 s
20ax	3H 1.09 s	3H 1.11 s	3H 0.97 s	3H 0.96 s	3H 0.89 s	3H 0.99 s	3H 0.83 s
21							
22		3H 2.03 s	3H 2.05 s	3H 2.07 s	3H 2.06 s	3H 1.94 s	3H 2.03 s

	δ_C [ppm], multiplicity (J in [Hz])[a]					
pos	**9**	**10**	**11**	**12**	**13**	**14**
1ax	0.93 m	0.70 dd (13.0, 3.8)	0.71 dt (13.1, 3.7)	0.98 dd (13.7, 3.6)	0.84 m	0.86 dt (13.6, 4.2)
1eq	1.49 m	1.45 m	1.46 m	1.59 m	1.51 m	1.51 m
2ax	1.56 m	1.32 m	1.34 m	1.68 m	1.54 m	1.54 m
2eq	1.56 m	1.52 m	1.53 m	2.34 dddd (13.9, 13.3, 12.8, 3.8)	1.54 m	1.58 m
3ax	4.43 dd (10.6, 5.7)	1.09 m	1.11 dd (9.2, 3.7)	4.77 dd (12.1, 4.7)	3.59 m	3.17 dd (11.1, 5.0)
3eq		1.34 m	1.34 m			
5ax	0.80 m	0.75 dd (12.0, 2.0)	0.75 dd (n.d.,2.0)	1.34 d (13.0)	0.82 m	0.72 dd (11.8, 1.9)
6ax	1.31 dt (12.1, 3.1)	1.47 m	1.24 ddd (12.3, 6.0, 2.5)	1.47 d (12.8)	1.30 m	1.29 dddd (13.0, 13.0, 12.6, 3.5)
6eq	1.48 m	1.47 m	1.51 m	1.65 m	1.30 m	1.53 m
7ax	1.45 m	1.42 m	1.44 m	1.42 d (15.0)	1.35 m	1.48 d (11.9)
7eq	1.45 m	1.41 m	1.44 m	1.26 dt (13.4, 3.7)	1.35 m	1.40 dt (13.0, 4.1)
9ax	1.11 m	1.14 brd (10.6)	1.17 ddd (n.d, 6.4, 1.7)	1.06 d (n.d.)	1.08 ddd (11.2, 7.3, 1.5)	1.10 ddd (11.2, 6.3, 1.2)
11a=α	1.90 ddd (14.7, 11.3, 3.0)	1.89 ddd (14.7, 11.3, 3.0)	1.94 ddd (15.2, 11.3, 3.2)	1.88 dt (12.8, 2.6)	1.86 ddd (14.5, 11.3, 3.1)	1.95 ddd (14.8, 11.4, 3.0)
11b=β	1.69 ddd (14.7, 7.0, 2.5)	1.69 ddd (14.7, 7.3, 2.5)	1.81 ddd (15.1, 6.4, 2.6)	1.63 m	1.64 ddd (14.5, 7.3, 2.4)	1.73 ddd (14.8, 6.3, 2.5)
12	0.79 m	0.79 dd (5.4, 2.7)	2.01 dt (8.3, 3.5)	0.55 br d (7.6)	0.57 dt (7.9, 2.4)	1.93 m
13	1.07 dd (8.1, 3.1)	1.06 dd (8.0, 3.0)	1.77 dt (8.5, 2.8)	0.79 dd (7.6,2.4)	0.79 dd (7.7, 3.3)	1.78 td (8.3, 2.5)
14a=β	2.08 d (12.0)	2.11 d (12.0)	2.22 d (12.1)	1.96 d (12.0)	2.03 d (11.9)	2.14 d (12.3)
14b=α	1.15 m	1.14 m	1.19 m	1.14 d (12.1)	1.14 ddd (11.7, 3.2, 1.7)	1.27 ddd (nd, 3.5, 1.7)
15a=β	1.58 d (11.3)	1.56 d (11.5)	1.81 d (11.6)	1.36 d (10.9)	1.38 d (11.2)	1.83 d (12.0)
15b=α	1.37 d (11.3)	1.39 d (11.5)	1.44 m	1.21 m	1.21 d (11.2)	1.47 d (12.0)
17a	3.61 d (11.3)	3.61 d (11.3)	8.92 s	3H 1.09 s	3H 1.11 s	3H, 0.95 s
17b	3.57 d (11.3)	3.57 d (11.3)				
18	3H 0.82 s	3H 0.82 s	3H 0.83s	4.19 d (11.5) 4.29 d (11.5)	3.38 d (10.4) 3.68 d (10.4)	3H, 0.92 s
19	3H 0.82 s	3H 0.78 s	3H 0.78 s		3H 0.86 s	3H, 0.75 s
20ax	3H 0.95 s	3H 0.93 s	3H 0.94 s	3H 0.94 s	3H 0.97 s	
21				(at C18) 3H 2.02 s		
22	3H 2.03 s			3H 2.00 s		

[a] nd = coupling constant not detectable.

Compounds **7** and **8** were also identified as diastereomers with a common molecular formula of $C_{22}H_{32}O_3$ (**7** *m/z* 345.2441 $[M + H]^+$ and **8** *m/z* 345.2423 $[M + H]^+$, respectively). ^{13}C NMR and HMBC experiments were congruent and consistent with an epimeric pair, which indicates an acetylated hydroxy group at C-3 for both compounds (**7**: carboxyl group at δ_C 170.28, oxymethine at δ_C 73.51; **8**: carboxyl group at δ_C 170.48, oxymethine δ_C 78.64). The most downfield signals present in the ^{13}C NMR spectra of **7** (δ_C 204.44) and **8** (δ_C 204.63) revealed the presence of a formyl functionality. Key HMBC correlations for **7** included ^3J-couplings from H-3 (δ_H 4.91, dd, $J = 11.3$, 5.1 Hz) to C-18 (δ_C 204.44) and to C-21 (δ_C 170.28), representing the carbonyl carbon of the acetyl residue. Additional correlations were observed for H-9 (δ_H 1.04, s) to C-1 (δ_C 36.80). Strong NOESY responses observed between H-5 (δ_H 1.31, m) and H-18 (δ_H 9.22, s) and between H-5 and H-3 indicated that the methyl group at C-19 as well as the acetylated hydroxy group at C-3 are β-oriented. Thus, the structure of **7** was established as *ent*-3β-acetoxytrachyloban-18-al, while compound **8** was identified as the C-4 epimer of **7**, namely, *ent*-3β-acetoxytrachyloban-19-al.

It is important to note that a molecular ion for **7** and **8** could not be detected by GC-MS. However, the absence of the molecular ion is a rare but well-known phenomenon in GC-MS.[18] Increased ion-source temperatures during the analysis may have accelerated molecular ion fragmentation, resulting in a low intensity of the molecular ion.

The molecular formula $C_{22}H_{34}O_3$, of **9** was deduced from EIHRMS, DEPT ^{13}C NMR (5 C, 5 CH, 8 CH_2, 4 CH_3, Table 1), and IR data (hydroxy group at 3277 cm^{-1}, carbonyl group at 1740 cm^{-1}). The NMR analytical data were similar to those of compounds **5** and **6**, indicating that **9** represents a dihydroxylated trachylobane with acetylation at C-3. A hydroxymethylene carbon (C-17) was identified on the basis of a signal at δ_C 67.73. Key HMBC correlations of **9** included ^3J-couplings from the geminal protons H-17a/b (H-17a δ_H 3.61, d, $J = 11.3$ Hz; H-17b, δ_H 3.57, d, $J = 11.3$ Hz) to C-15 (δ_C 45.62) as well as to C-13 (δ_C 22.07). Thus, the structure of **9** was established as *ent*-3β-acetoxy-17-hydroxytrachylobane.

A molecular formula of $C_{20}H_{32}O$ for compound **10** was determined by EIHRMS analysis ($[M]^+$ 288.2451). The IR spectrum revealed a hydroxy absorption at 3277 cm^{-1} similar to **3**. The ^{13}C NMR spectrum exhibited 20 carbon resonances, assigned by DEPT experiments to four quaternary carbons, four methines, nine methylenes, and three methyls (Table 1). Together with a single hydroxy group, this accounted for the expected 32 protons. The carbon of the hydroxylated methylene substituent at C-17 gave a signal at δ_C 67.93, and its corresponding protons were identified at δ_H 3.57 (H-17b, d, $J = 11.3$ Hz) and δ_H 3.61 (H-17a, d, $J = 11.3$ Hz). Previously observed key signals for the trachylobane skeleton such as those for the cyclopropane ring (H-12 δ_H 0.79 dd, $J = 5.4$, 2.7 and H-13 δ_H 1.07 dd, $J = 8.1$, 3.1 Hz) were also detected. However these signals were shifted downfield due to the presence of an oxymethylene group attached to C-16. Key HMBC correlations observed for **10** included ^3J-couplings from the geminal protons H-17a and H-17b to both C-15 (δ_C 45.85) and C-13 (δ_C 22.19). On the basis of these results, structure **10** could be established as 17-hydroxytrachylobane.

The HREIMS of compound **11** supported a molecular formula of $C_{20}H_{30}O$ (*m/z* $[M + H]^+$ 287.2011). ^1H and ^{13}C NMR experiments revealed the presence of a trachylobane skeleton functionalized with a formyl group at C-17 (δ_C 201.08), which was confirmed by a strong IR absorption at 1677 cm^{-1}. Compared with **10**, the ^{13}C NMR data of **11** revealed a high-field shift of C-15 (δ_C 40.78) and a low-field shift of C-16 (δ_C 41.88). The latter could be explained by the presence of a formyl group at C-16. Key HMBC correlations were observed and included ^3J-couplings from H-17 (δ_H 8.92, s) to C-15 (δ_C 40.78) as well as a ^2J-coupling between H-17 and C-16 (δ_C 41.88). Taking the additional HMBC and H,H-COSY data into account, the spectroscopic data of compound **11** were consistent with *ent*-trachyloban-17-al.

Compound **12** was obtained as yellow solid with a molecular formula of $C_{24}H_{33}O_6$ as determined by MS (*m/z* = 418). Its structure could be deduced from the 1- and 2-D NMR experiments. In this process, the presence of two acetylated hydroxy groups at C-3 (δ_C 73.00) and C-18 (δ_C 62.53) as well as a carboxyl group at C-19 (δ_C 176.93) could be identified from correlations observed in the HMBC experiment. These and other results suggested structure **12** as *ent*-3β,18α-diacetoxy-19-trachylobanoic acid.

EIHRMS analysis of **13** displayed an exact mass of *m/z* $[M]^+$ 304.2404 and suggested a molecular formula of $C_{20}H_{32}O_2$. ^{13}C NMR data revealed the presence of primary (C-18, δ_C 72.05) and secondary (C-3, δ_C 77.10) alcohol functionalities, but no additional functionalities. The position of these two hydroxy groups could be deduced from HMBC and NOESY correlations. Similar to structures **1** and **5**, one hydroxy group was located at C-3, whereas the second hydroxy group was attached to C-18. Key NOESY correlation cross-peaks for **13** were observed between H-3 (δ_H 3.59, m) and H-19 (δ_H 0.86, s) as well as between H-19 and H-20 (δ_H 0.97 s). Thus, the structure of **13** was assigned to *ent*-3β,18α-dihydroxytrachylobane.

Compound **14** was obtained as a white, amorphous powder. Its molecular mass ($[M]^+$ 318.2195) suggested a molecular formula of $C_{20}H_{30}O_3$. The ^{13}C NMR spectrum revealed the presence of 20 carbon resonances, assigned by HMBC and DEPT experiments to four quaternary, five methine, seven methylene, and three methyl carbons. These, plus one hydroxy group and one carboxylic proton accounted for the expected 30 protons. A secondary alcohol functionality was identified by a characteristic shift of H-3 at δ_H 3.17 (dd, $J = 11.1$, 5.0 Hz) and its corresponding carbon (C-3 δ_C 79.98). The ^{13}C NMR data further showed the typical signals associated with the trachylobane ring skeleton functionalized with a carboxyl group at C-16 (δ_C 180.83). Thus, compound **14** was identified as *ent*-3β-hydroxy-17-trachylobanoic acid.

Analysis of the ^1H NMR spectrum by computational full-spin analysis of **1** was performed with the PERCH iteration software and confirmed the full assignments of the ^1H resonances including their multiplicities. The concept and workflow of full-spin analysis has recently been reported for the natural products β-pinene and huperzine A.[19,23] In brief, the analysis determines all spin parameters (δ, ^nJ) of all protons and consists of an iterative minimization of the difference between spin-simulated and experimental spectra. Despite minor limitations associated with the achievable signal purity of **1** (overlap with minor sample components, particularly in the high-field region of the ^1H NMR spectrum), the observed and simulated spectra showed very good congruence (Figure 1). The coupling constants deduced by ^1H NMR spectroscopic iteration (J_{it}) reflect the "true" values, including higher order effects, and are summarized in Table 4. Numerous small coupling constants ($J \ll 1$ Hz) in **1** could not be directly determined from the 500 MHz ^1H NMR spectrum due to higher order spin coupling effects. This information became accessible by spectroscopic iteration of the 900 MHz ^1H NMR data, which allowed the analysis of signal splittings that were "hidden" in the sometimes complex signal multiplicities. As many small spin−spin couplings were found to be due to ^4J *W*-type pathways, their presence could be used as additional constraint when defining the constitution and relative configuration of **1**. Figures 2 and 3 show a model of the conformationally averaged $CDCl_3$ solution structure of **1** that is compatible with all the ^1H NMR evidence, including the ^3J Karplus constraints for torsion angles between vicinal protons. Unlike the two six-membered rings A and B, both of which are present in a chair conformation, ring C exhibits distortions due to its connectivity with the additional three-, five-, and six-membered rings. Thus, the H,H-coupling patterns in ring C are very complex. The H-12 signal (Figure 3) is a particularly characteristic case: Full-spin analysis

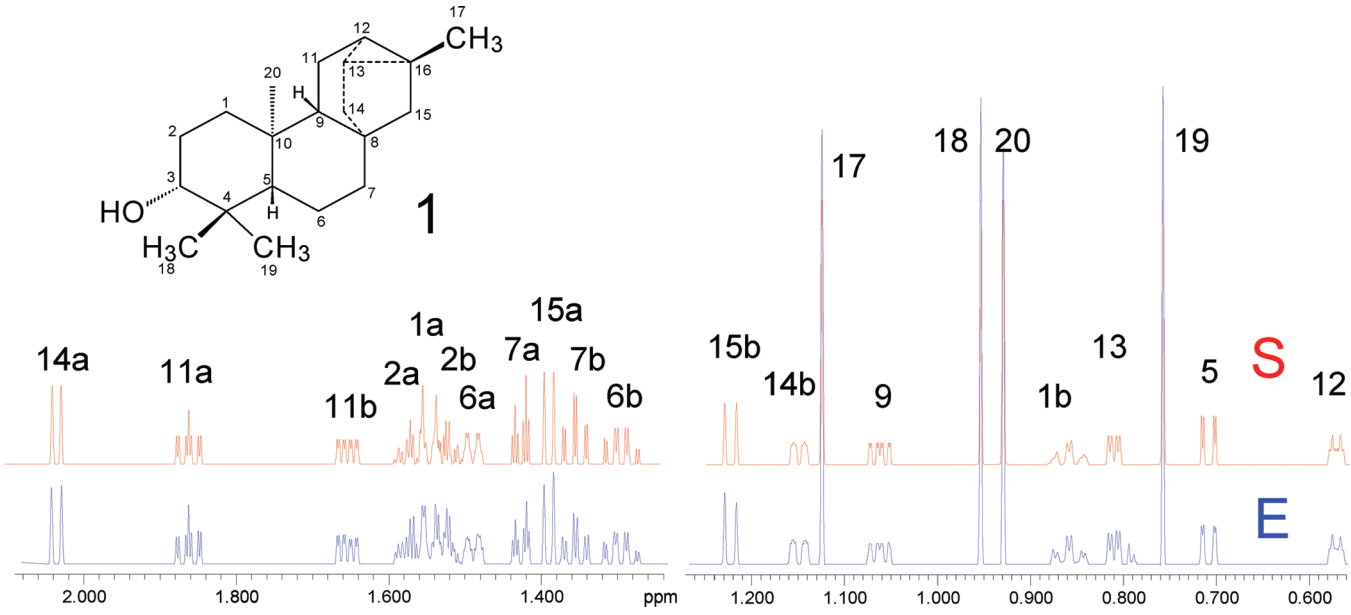

Figure 1. Experimental (E) and simulated (S) ^{1}H NMR spectrum of **1**.

Table 3. Anti-TB Activities of the Isolated Trachylobanes against *M. tuberculosis* $H_{37}Rv$ (MABA assay)

		MIC_{90}[a]	
cpd	name	μg/mL	μM
1	*ent*-3β-hydroxytrachylobane	61	212
2	*ent*-trachyloban-3-one	50	173
3	*ent*-3β-acetoxytrachylobane	111	337
4	*ent*-3β-acetoxy-18-hydroxytrachylobane	>128	>370
5	*ent*-18α-acetoxy-3β-hydroxytrachylobane	>128	>370
6	*ent*-3β-acetoxy-19-hydroxytrachylobane	59	171
7	*ent*-3β-acetoxytrachyloban-18-al	>128	>371
8	*ent*-3β-acetoxytrachyloban-19-al	>128	>371
9	*ent*-3β-acetoxy-17-hydroxytrachylobane	n.t.	n.t.
10	*ent*-17-hydroxytrachylobane	>128	446
11	*ent*-trachyloban-17-al	24	85
12	*ent*-3β,18α-diacetoxy-19-trachylobanoic acid	>128	>306
13	*ent*-3β,18α-dihydroxytrachylobane	n.t.	n.t.
14	*ent*-3β-hydroxy-17-trachylobanoic acid	>128	>402
positive control	rifampin	<0.12	<0.15

[a] n.t. not tested due to sample limitations.

confirmed the observed ^3J-couplings between H-12 and H-13 (J_{it} = 7.80 Hz) as well as couplings between H-12 and H11a (J_{it} = 2.92 Hz) and between H12 and H11b (J_{it} = 2.58 Hz). Very small couplings between H-12 and the methyl group at C-16 (J_{it} = 0.70 Hz) as well as a weak ^4J *W*-coupling between H-12 and H-9 (J_{it} = 0.20 Hz) could be extracted. As noted earlier, these small coupling constants (J < 1 Hz) could not be directly measured in the experimental ^{1}H signal shape and/or splitting pattern and require optimized postacquisition processing and subsequent iterative analysis. The conformationally averaged solution structure of **1** was further characterized based on the presence and magnitude of *J*-couplings, following general Karplus relationships. To provide examples for ring C, H-12 and H-13 share a ^3J-coupling of J_{it} = 7.80 Hz, indicating that they are located in the same plane ($\phi \approx 0°$) and not *trans*-diaxial ($\phi \approx 180°$). In contrast, the CH bonds of both protons H-11a and H-11b are out of the plane relative to H-12, which explains their smaller ^3J-couplings of J_{it} = 2.92 and J_{it} = 2.68 Hz, respectively. Because these vicinal *J*-values are almost equal in magnitude, the signal of H-12 has the characteristic first-order shape of a td, combining two small and one big coupling. Finally, the very weak ^4J-coupling between H-12 and H-9 (J_{it} = 0.28 Hz) confirms the skewed *W*-like geometry of the connecting bonds. However, the C-17 methyl protons show a significant four-bond correlation to H-12 (J_{it} = 0.70 Hz), which is typical for bridgehead methyl groups in highly constrained oligocyclic small molecules[19] such as the cyclopropane partial structure in ring C.

The isolates were evaluated in the MABA assay[20] for their anti-TB activity against virulent *M. tuberculosis* H37R*v*. In this assay, current standard anti-TB drugs exhibit MICs in the range 0.1 to 128 μg/mL, which were chosen as test concentrations. The highest antimycobacterial potential was observed for **11** (MIC: 24 μg/mL or 85 μM) followed by **6** (MIC: 59 μg/mL or 171 μM), **2** (MIC: 50 μg/mL or 173 μM), **1** (MIC: 61 μg/mL or 212 μM), and **3** (MIC: 111 μg/mL or 337 μM). Compounds **4**, **5**, **7**, **8**, **10**, **12**, and **14** showed MICs > 128 μg/mL and were, thus, considered to be inactive. Compounds **9** and **13** could not be tested due to sample limitations. The nine compounds that were biologically evaluated in this study did not provide sufficient chemical diversity to enable the identification of the anti-TB pharmacophore of the trachylobanes. A summary of the activity profile of all isolated trachylobane diterpenes is given in Table 3. Overall, while the *Jungermannia* trachylobanes exhibited moderate antimycobacterial activity, the activity of four of the new compounds falls into the range of clinically used anti-TB drugs and warrants further investigation of the anti-TB potential of the compound class. Separate studies will be necessary to address possible synergistic effects and the potential of analoging to search for improvements in their observed activity.

Experimental Section

General Experimental Procedures. Optical rotation was recorded on a Perkin-Elmer 241 polarimeter in $CHCl_3$. IR spectra were measured on a Perkin-Elmer 257 spectrometer and on a Bio Rad FTS 3000 MX Excalibur FT-IR spectrometer. UV spectra were recorded on a Perkin-Elmer Lambda 2. All NMR experiments were performed on a Bruker DRX 500 NMR spectrometer. NMR spectra were recorded in $CDCl_3$. Chemical shifts are given in parts per million (ppm) on the δ scale relative to the solvent peaks $CHCl_3$ at δ_H 7.25 and $CDCl_3$ at δ_C 77.0. ^{13}C multiplicities were determined using the DEPT-135 pulse sequence. The 900 MHz ^{1}H NMR spectrum of **1** was recorded on a Bruker Avance 900 MHz NMR spectrometer, which was equipped with a 5 mm indirect ^{1}H, ^{13}C, ^{15}N triple resonance cryoprobe (TCI) accessory. Full-spin simulation analysis of the 900 MHz spectrum of **1** was performed using PERCH spin simulation software from PERCH Solutions Ltd., Kuopio, Finland. High-resolution mass spectrometry, EIMS, CIMS, and DCIMS data were recorded on a Finnigan MAT 90 spectrometer. GC-MS was performed with a Hewlett-Packard G1800A GCD

Table 4. Matrix of the Coupling Orders (right above diagonal) and *J*-Values (left below diagonal) of the 47 H,H-Coupling Constants in **1** Determined by Spectroscopic Iteration (J_{it})

	mult.	δ_H	1a	1b	2a	2b	3	5	6a	6b	7a	7b	9	11a	11b	12	13	14a	14b	15a	15b	17	18	19	20
1ax=α	ddd/m	1.547[a]	*	^2J	^3J	^3J																			^4J
1eq=β	ddd/m	0.858	−13.71	*	^3J	^3J	^4J																		^4J
2ax=β	dddd/m	1.571[a]	3.4[a]	13.73	*	^2J	^3J																		
2eq=α	dddd/m	1.524[a]	2.5[a]	3.68	−13.00	*	^3J																		
3ax=α	dd/m	3.179		0.75	4.10	10.40	*																^4J	^4J	
5ax=α	dd	0.708						*	^3J	^3J													^4J	^4J	^4J
6ax=β	dddd/m	1.490						11.95	*	^2J	^3J	^3J													
6eq=α	dddd/m	1.295						2.09	−13.10	*	^3J	^3J													
7eq=β	dddd/m	1.426							3.00	13.30	*	^2J													
7ax=α	dddd/m	1.355							3.30	3.30	−13.10	*													
9ax=α	ddd/m	1.062											*	^3J	^3J	^4J	^5J		^4J	^4J	^4J				
11a=α	ddd	1.862											11.24	*	^2J	^3J									
11b=β	ddd	1.654											7.19	−14.60	*	^3J									
12=α	td/ddd	0.571											0.20	2.92	2.58	*	^3J								
13	dd	0.810											0.20			7.80	*	^3J	^3J			^4J			
14a=α	(br)d	2.036															0.84	*	^2J	^3J	^3J				
14b=β	ddd	1.149											1.77				3.29	−11.40	*	^3J	^3J				
15a=β	d	1.390											<0.1					0.94	0.63	*	^2J	^4J			
15b=α	d	1.223											0.20					0.94	0.63	−11.30	*	^4J			
17	dd	1.124														0.70	0.60			0.36	0.36	*			
18eq=α	dd	0.953					0.26		0.20														*		
19ax=β	s	0.757					<0.1		<0.1															*	
20ax=β	(br)d	0.929	0.72	0.57					<0.1				0.30												*

[a] Due to interference with impurities, some signals could not be fully iterated.

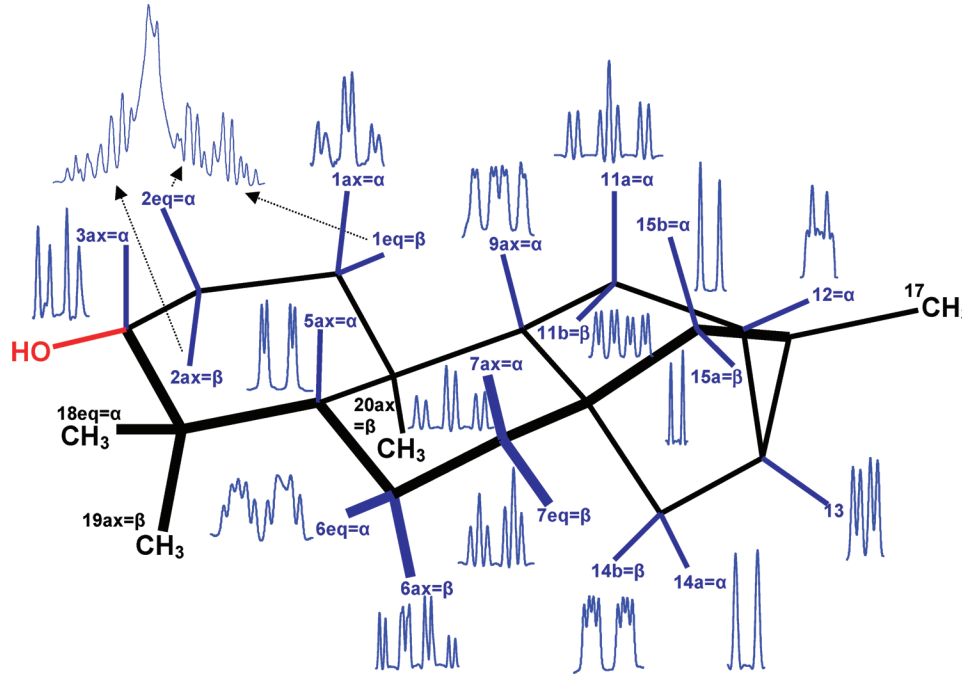

Figure 2. At 900 MHz, with the exception of the methylene protons at C-2, the ^{1}H NMR signals of **1** permit a near first-order interpretation of their multiplicities. Full-spin analysis by spectroscopic iteration and simulation with the PERCH software tool accounted for all higher order spin coupling effects in the spectrum. Following the general Karplus relationship, the observed ^3J-coupling patterns were aligned with the relative configurations in the depicted conformer. The observation of numerous *W*-type (^4J) couplings provided additional constraints for the conformationally averaged molecule in $CDCl_3$ solution. While some of these long-range couplings were relatively large, such as the 1.8 Hz ^4J between H-9 and H-14b, most required a full-spin analysis for extraction of the coupling information and constants.

system using He (60 Kpa, 1 mL/min) as the carrier gas. Samples were analyzed on a HP-5 column (15 m × 0.25 mm i.d., 0.25 μm film).

Silica gel (LiChroprep, 40−63 μm, LiChroprep, 15 μm) and diol-modified silica gel (LiChroprep diol, 40−63 μm LiChroprep diol, 15 μm) were used for VLC and purchased from Merck, Darmstadt, Germany. TLC was performed on silica gel (silica gel 60 F_{254}), reversed-phase C18 (HPTLC plates, RP18, F_{254}), and diol- and cyano-modified silica (HPTLC plates, RP18, F_{254}) also purchased from Merck, Darmstadt, Germany. HPLC separations were performed using a Waters 600 E multisolvent delivery system equipped with a Merck-Hitachi L-4000 UV detector.

Plant Material. *Jungermannia exsertifolia* subsp. *cordifolia* was collected at around 2400 m altitude in the Alps (Switzerland) during July 2003. A voucher specimen (#6395) is deposited in the Herbarium Saar.

Extraction and Isolation. The extraction scheme followed the standard procedure of our group.[21] Air-dried and ground plant material (642 g) of *J. exsertifolia* was extracted with distilled CH_2Cl_2. The crude extract was subjected to rotary evaporation under reduced pressure at 40 °C, yielding 22.33 g of dry extract. The latter was fractionated by VLC applying an *n*-hexane−EtOAc−MeOH gradient. Nine subfractions were obtained. Fr. 2 (1.76 g) was chromatographed on diol silica gel by preparative HPLC (LiChrospher 100 diol, 5 μm, 250 × 8 mm,

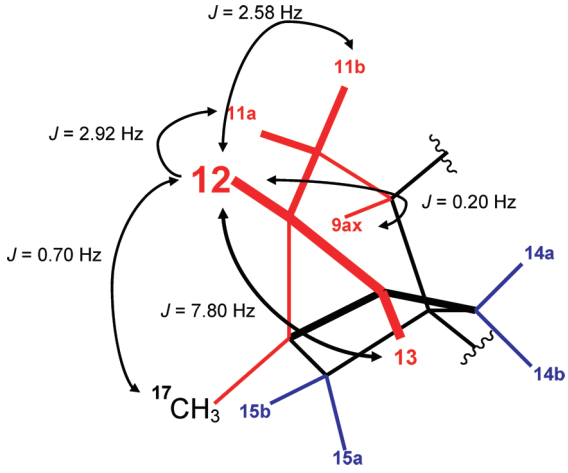

Figure 3. The complex ^{1}H,^{1}H coupling pathways between the trachylobane bridgehead proton, H-12, and its H−H coupling partners in the C ring of **1** demonstrate the rigidity of the molecule and are in agreement with the findings of multiple long-rang couplings found in oligocyclic compounds such as the monoterpene *β*-pinene[19] or the alkaloid huperzine A.[23]

mobile phase 5.0 mL/min *n*-hexane−EtOAc, 98.5:1.5), yielding 15 mg of **3** ($t_R \approx 6$ min), 10 mg of **2** ($t_R \approx 7.5$ min), and two subfractions (fr. 2.1: $t_R \approx 11$ min and fr. 2.2: $t_R \approx 12$ min). Further HPLC separation (Spherisorb CN, 5 mm, *n*-hexane−EtOAc, 90:10, 1.5 mL/min) of fr. 2.1 yielded 10 mg of **8** ($t_R \approx 9$ min) and 15 mg of **11** ($t_R \approx 10$ min). HPLC separation (LiChrospher 100 Si, 5 *μ*m, *n*-hexane−EtOAc, 90:10, flow 1.5 mL/min) of fr. 2.2 resulted in the isolation of **7** ($t_R \approx 12$ min, 5 mg).

Fraction 3 (3.13 g) was chromatographed on Sephadex LH-20 [MeOH−CH_2Cl_2 (1:1)] giving four subfractions (fr. 3.1−3.4). Further separation of fr. 3.4 (HPLC, LiChrospher 100 diol, 5 *μ*m, *n*-hexane−EtOAc, 95:5) yielded **1** (20 mg) and **10** (4 mg).

Fraction 4 (2.0 g) was chromatographed on diol via preparative HPLC (LiChrospher 100 diol, 5 *μ*m, 250 × 8 mm, mobile phase 5.0 mL/min *n*-hexane−EtOAc, 90:10), giving seven subfractions (fr. 4.1−4.7). Separation of fr. 4.2 using HPLC (LiChrospher 100 Si, 5 *μ*m, *n*-hexane−EtOAc, 90:10, flow rate 1.8 mL/min) yielded 8 mg of **4** ($t_R \approx 19$ min) and 9 mg of **6** ($t_R \approx 26$ min).

Fraction 5 (951 mg) was chromatographed on silica gel via VLC using an *n*-hexane−EtOAc gradient producing five subfractions (fr. 5.1−5.5). Further purification of fr. 5.2 (61 mg) by HPLC (LiChrospher 100 diol, 5 *μ*m, *n*-hexane−EtOAc, 90:10, flow rate 1.9 mL/min) yielded 10 mg of **5** ($t_R \approx 7$ min). Fraction 5.4 (227 mg) was chromatographed on silica gel via VLC using an *n*-hexane−EtOAc gradient, giving four subfractions (fr. 5.4.1−5.4.4). Further purification of fr. 5.4.3 (43 mg) by HPLC (LiChrospher 100 diol, 5 *μ*m, *n*-hexane−EtOAc, 90:10, flow rate 1.9 mL/min) yielded 10 mg of **9** ($t_R \approx 7$ min).

Fraction 8 (3.33 mg) was chromatographed on silica gel via VLC using an *n*-hexane−EtOAc gradient, yielding seven subfractions. (fr. 8.1−8.7). Further purification of fr. 8.2 (276 mg) by HPLC (LiChrospher 100 diol, 5 *μ*m, *n*-hexane−EtOAc, 97.5:2.5, flow rate 1.8 mL/min) yielded 185 mg of **12** ($t_R \approx 15$ min). Further purification of fr. 8.3 (301 mg) using HPLC (LiChrospher 100 diol, 5 *μ*m, *n*-hexane−EtOAc, 97.5:2.5, flow rate 1.8 mL/min) yielded 7 mg of **13** ($t_R \approx 18$ min) and 8 mg of **14** ($t_R \approx 25$ min).

***ent*-3*β*-Hydroxytrachylobane (1):** white powder $[\alpha]_D^{20}$ −44.1 (*c* 0.49, $CHCl_3$;); IR ν_{max} 3275, 2928, 2859, 2360, 1710, 1442, 1385, 1038, 1002 cm^{-1}; ^{1}H NMR Table 2; ^{13}C NMR Table 1; GC-MS *m/z* [M]$^+$ 288 (100.0), 273 (20.1), 255 (27.9), 232 (39.1), 217 (23.8), 199 (19.5), 173 (11.8), 159 (13.2), 148 (11.1), 147 (19.5), 145 (19.8), 139 (12.3), 136 (15.8), 135 (38.2), 134 (24.4), 133 (24.7), 132 (12.8), 131 (22.7), 123 (19.9), 121 (30.9), 120 (18.9), 119 (55.6), 117 (20.8), 116 (19.2), 109 (24.9), 108 (12.2), 107 (47.5), 106 (44.1), 105 (87.5), 95 (28.3), 94 (22.6), 93 (74.5), 92 (31.7), 91 (85.6), 83 (13.4), 82 (11.8), 81 (37.3), 80 (21.0), 79 (54.3), 78 (10.6), 77 (34.9), 71 (16.7), 69 (42.1), 67 (34.8), 65 (10.0), 57 (91.0), 55 (53.5), 53 (18.2); (EI) HR-MS *m/z* 288.2404 (calcd for $C_{20}H_{32}O$, 288.2453).

***ent*-Trachyloban-3-one (2):** white powder $[\alpha]_D^{20}$ −19.6 (*c* 0.28, $CHCl_3$); IR ν_{max} 2916, 2849, 1738, 1703, 1458, 1381, 1246, 1174, 1109, 1007 cm^{-1}; ^{1}H NMR Table 2; ^{13}C NMR Table 1; GC-MS *m/z* [M]$^+$ 286 (100.0), 271 (20.9), 230 (23.9), 229 (9.1), 215 (18.3), 201 (10.0), 200 (12.7), 187 (10.0), 173 (11.0), 159 (18.3), 147 (12.2), 145 (23.8), 139 (9.9), 135 (10.8), 134 (10.2), 133 (16.9), 132 (9.0), 130 (23.3), 125 (16.6), 123 (8.4), 121 (12.7), 120 (9.7), 119 (39.9), 117 (11.2), 116 (16.3), 109 (12.5), 107 (31.1), 106 (25.7), 105 (74.2), 98 (21.3), 97 (8.8), 95 (17.3), 94 (12.8), 93 (59.0), 92 (20.8), 91 (71.6), 83 (14.4), 81 (30.9), 80 (16.6), 79 (46.6), 77 (31.2), 69 (35.6), 67 (34.1), 65 (9.9), 57 (8.4), 56 (8.3), 55 (79.7), 53 (17.4).

***ent*-3*β*-Acetoxytrachylobane (3):** orange gum; $[\alpha]_D^{20}$ −39.4 (*c* 0.63, $CHCl_3$); IR ν_{max} 2938, 1719, 1463, 1440, 1369, 1244, 1032, 1004 cm^{-1}; ^{1}H NMR Table 2; ^{13}C NMR Table 1; GC-MS *m/z* [M]$^+$ 330 (100.0), 315 (11.6), 288 (10.1), 275 (10.5), 274 (51), 270 (13.2), 259 (9.8) 256 (11.7), 255 (55.4), 227 (10.7), 215 (7.9), 214 (16.7), 200 (9.1), 199 (39.1), 189 (8.3), 188 (15.0), 187 (10.3), 185 (7.8), 175 (10.7), 171 (10.2), 161 (10.8), 159 (15.9), 157 (8.4), 149 (8.5), 148 (10.7), 147 (20.3), 146 (11.2), 145 (20.3), 143 (7.8), 137 (9.2), 136 (20.3), 135 (44.3), 134 (29.3), 133 (30.3), 132 (18.3), 131 (25.1), 123 (29.7), 122 (12.1), 120 (23.5), 119 (62.3), 117 (25.3), 116 (19.8), 109 (28.3), 108 (12.0), 107 (48.3), 106 (45.4), 105 (96.4), 95 (34.0), 94 (22.8), 92 (31.6), 91 (83.0), 83 (13.5), 82 (16.3), 80 (21.2), 79 (53.5), 78 (9.1), 77 (30.5), 71 (8.7), 69 (58.4), 67 (31.4), 57 (10.3), 53 (13.5); (EI) HR-MS *m/z* 330.2555 (calcd for $C_{22}H_{34}O_2$, 330.2559).

***ent*-3*β*-Acetoxy-18-hydroxytrachylobane (4):** white solid; $[\alpha]_D^{20}$ −11.3 (*c* 0.28 $CHCl_3$); IR ν_{max} 3515, 2930, 1717, 1443, 1376, 1269, 1055, 1029 cm^{-1}; ^{1}H NMR Table 2; ^{13}C NMR Table 1; GC-MS *m/z* [M]$^+$ 346 (8.7), 286 (11.9), 257 (13.9), 256 (54.1), 255 (11.7), 253 (8.1), 241 (34.6), 227 (8.7), 201 (13.1), 200 (8.7), 199 (9.1), 185 (11.8), 175 (28.6), 174 (9.4), 171 (9.5), 161 (8.3), 159 (19.8), 157 (11.1), 147 (14.1), 146 (8.7), 145 (23.6), 143 (9.6), 138 (17.4), 135 (9.3), 134 (13.9), 133 (28.4), 132 (14.6), 131 (25.0), 122 (12.6), 119 (48.0), 117 (26.3), 116 (16.9), 109 (16.9), 108 (12.5), 107 (54.4), 106 (38.1), 105 (100.0), 95 (28.7), 94 (15.3), 93 (68.1), 91 (68.8), 81 (37.1), 80 (11.6), 79 (45.2), 77 (24.1), 69 (20.2), 67 (24.7), 61 (21.3), 57 (16.2), 55 (42.7), 53 (11.2); (EI) HR-MS *m/z* 346.2523 (calcd for $C_{22}H_{34}O_3$, 346.2508).

***ent*-18-α-Acetoxy-3*β*-hydroxytrachylobane (5):** white solid; $[\alpha]_D^{20}$ −15.5 (*c* 0.39 $CHCl_3$); IR ν_{max} 3265, 2926, 2860, 1744, 1463, 1443, 1381, 1366, 1238, 1035, 1010 cm^{-1}; ^{1}H NMR Table 2; ^{13}C NMR Table 1; GC-MS *m/z* [M]$^+$ 346 (8.2), 286 (11.1), 257 (10.4), 256 (39.4), 255 (9.7), 241 (25.1), 201 (10.8), 185 (10.1), 175 (28.0), 173 (12.1), 171 (9.1), 159 (19.0), 157 (11.1), 147 (13.2), 138 (12.0), 134 (8.9), 133 (25.6), 132 (13.6), 131 (23.6), 122 (11.3), 121 (23.9), 119 (47.6), 117 (25.4), 116 (16.5), 109 (15.7), 108 (11.5), 107 (55.1), 106 (39.4), 105 (100.0), 95 (26.2), 94 (14.7), 93 (68.5), 92 (22.2), 91 (72.0), 81 (35.6), 80 (12.7), 79 (47.4), 77 (25.8), 69 (20.6), 67 (26.2), 61 (24.6), 57 (18.3), 55 (45.2), 53 (12.4); (EI) HR-MS *m/z* 346.2508 (calcd for $C_{22}H_{34}O_3$, 346.2508).

***ent*-3*β*-Acetoxy-19-hydroxytrachylobane (6):** colorless oil; $[\alpha]_D^{20}$ −27.0 (*c* 0.12 $CHCl_3$); IR ν_{max} 3515, 2930, 1717, 1443, 1376, 1269, 1055, 1029 cm^{-1}; ^{1}H NMR Table 2; ^{13}C NMR Table 1; GC-MS *m/z* [M]$^+$ 346 (14.1), 286 (15.4), 255 (9.5), 229 (10.4), 175 (38.7), 174 (12.1), 173 (11.1), 159 (18.5), 157 (8.6), 147 (12.3), 135 (8.6), 134 (13.0), 133 (22.0), 132 (16.4), 130 (21.7), 122 (8.7), 121 (23.7), 120 (15.3), 119 (48.8), 117 (30.3), 116 (15.6), 109 (13.9), 108 (12.6), 106 (42.2), 105 (100.0), 95 (24.1), 94 (15.7), 93 (60.6), 92 (19.4), 91 (60.0), 81 (32.5), 80 (10.2), 79 (38.8), 77 (20.8), 69 (17.5), 67 (21.5), 61 (16.7), 57 (14.5), 55 (35.9), 53 (9.5); (EI) HR-MS (EI) *m/z* 346.2508 (calcd for $C_{22}H_{34}O_3$, 346.2508).

***ent*-3*β*-Acetoxytrachyloban-18-al (7):** white gum; $[\alpha]_D^{20}$ −27.4 (*c* 0.15 $CHCl_3$); IR ν_{max} 3443, 2927, 1739, 1721, 1445, 1371, 1247, 1029 cm^{-1}; ^{1}H NMR Table 2; ^{13}C NMR Table 1; GC-MS *m/z* 257 (18.0), 256 (90.7), 242 (19.0), 241 (97.5), 227 (16.9), 227 (16.9), 201 (25.9), 200 (12.4), 185 (26.3), 173 (8.5), 171 (11.1), 161 (8.8), 159 (18.5), 157 (11.8), 147 (13.2), 145 (30.0), 143 (11.2), 138 (28.2), 136 (8.8), 135 (9.0), 134 (15.6), 133 (37.3), 132 (11.4), 131 (27.9), 128 (9.0), 123 (10.9), 122 (30.4), 120 (27.5), 119 (53.0), 117 (21.5), 116 (19.2), 109 (24.7), 108 (13.4), 107 (52.4), 106 (34.7), 105 (100.0), 95 (36.1), 94 (19.2), 93 (77.4), 92 (24.7), 91 (85.5), 81 (39.6), 80 (14.5), 79 (57.3), 78 (9.4), 77 (32.5), 69 (14.2), 67 (26.9), 65 (8.6), 61 (16.6), 55 (48.7), 53 (15.7); (CI) HR-MS [M + H]$^+$ *m/z* 345.2441 (calcd for $C_{22}H_{33}O_3$, 345.2351).

***ent*-3*β*-Acetoxytrachyloban-19-al (8):** colorless oil; $[\alpha]_D^{20}$ −33.4 (*c* 0.15 $CHCl_3$); IR ν_{max} 3455, 2945, 2913, 2853, 2360, 1732, 1466, 1438,

1376, 1251, 1225, 1029 cm^{-1}; ^1H NMR Table 2; ^{13}C NMR Table 1; GC-MS *m/z* (rel int) 304 (15.4), 301 (9.2), 285 (9.8), 244 (14.2), 243 (16.5), 200 (12.0), 198 (9.2), 173 (8.9), 159 (13.8), 158 (8.5), 156 (13.7), 149 (9.2), 146 (11.5), 145 (10.7), 144 (15.4), 143 (15.5), 134 (13.7), 133 (12.0), 132 (21.8), 130 (28.3), 122 (9.1), 121 (28.7), 120 (26.4), 118 (43.4), 117 (21.3), 117 (23.2), 114 (15.5), 109 (12.1), 107 (12.1), 106 (68.9), 105 (100.0), 103 (14.0), 95 (39.4), 94 (33.2), 93 (50.1), 92 (29.3), 91 (92.9), 81 (24.1), 79 (15.3), 78 (49.8), 77 (46.8), 67 (20.5), 55 (40.3); (CI) HR-MS (CI) $[M + H]^+$ *m/z* 345.2423 (calcd for $C_{22}H_{33}O_3$, 345.2351).

***ent*-3*β*-Acetoxy-17-hydroxytrachylobane (9):** white gum; ^1H NMR Table 2; ^{13}C NMR Table 1; (EI) HR-MS *m/z* 346.2523 (calcd for $C_{22}H_{34}O_3$, 346.2508).

***ent*-17-Hydroxytrachylobane (10):** white gum; $[\alpha]_D^{20}$ −29.2 (*c* 0.11 $CHCl_3$); IR ν_{max} 2921, 2860, 1683, 1462, 1440, 1385, 1368, 1015 cm^{-1}; ^1H NMR Table 2; ^{13}C NMR Table 1; GC-MS *m/z* $[M]^+$ 288 (42.0), 273 (33.5), 257 (15.1), 255 (13.2), 217 (22.8), 216 (35.1), 201 (30.9), 173 (8.6), 159 (10.0), 147 (14.4), 145 (19.2), 143 (9.0), 137 (18.8), 132 (15.6), 131 (27.4), 124 (8.1), 123 (45.5), 121 (21.1), 120 (8.6), 119 (24.5), 117 (37.7), 115 (12.7), 109 (29.7), 107 (28.3), 106 (17.3), 105 (49.8), 103 (15.8), 102 (8.1), 97 (14.6), 96 (10.6), 95 (42.4), 94 (12.5), 93 (42.0), 92 (31.5), 91 (100.0), 83 (22.8), 82, (17.0), 81 (52.5), 80 (15.8), 79 (79.8), 78 (12.7), 77 (33.3), 71 (11.1), 70 (8.3), 69 (88.7), 68 (15.1), 67 (51.8), 65 (11.4), 57 (65.1), 56 (22.0), 55 (75.8), 53 (19.0); (EI) HR-MS *m/z* 288.2451 (calcd for $C_{20}H_{32}O$, 288.2453).

***ent*-Trachyloban-17-al (11):** white gum; $[\alpha]_D^{20}$ −62.7 (*c* 0.19 $CHCl_3$); IR ν_{max} 3455, 2927, 2864, 1736, 1677, 1462, 1442, 1387, 1367, 1260, 1044, 1014 cm^{-1}; ^1H NMR Table 2; ^{13}C NMR Table 1; GC-MS *m/z* $[M]^+$ 286 (58.7), 272 (8.6), 271 (43.5), 228 (9.0), 215 (8.4), 201 (11.9), 190 (8.5), 189 (21.0), 175 (9.2), 173 (10.7), 163 (9.6), 162 (14.1), 161 (10.8), 159 (9.2), 149 (13.5), 148 (19.6), 147 (16.8), 145 (18.8), 143 (9.9), 137 (16.1), 136 (8.1), 135 (11.9), 134 (11.1), 133 (23.4), 131 (21.9), 128 (16.3), 127 (9.8), 124 (23.9), 123 (88.4), 122 (20.2), 120 (14.6), 119 (26.9), 117 (29.5), 114 (15.0), 109 (38.8), 108 (21.4), 107 (30.9), 106 (11.3), 105 (45.6), 103 (11.5), 102 (10.8), 97 (11.5), 96 (11.9), 93 (32.0), 92 (26.5), 91 (100.0), 83 (19.0), 82 (32.7), 81 (57.0), 80 (15.2), 79 (82.4), 78 (16.0), 77 (45.0), 70 (9.8), 69 (92.5), 68 (22.5), 67 (65.3), 66 (9.2), 65 (16.1), 57 (19.4), 56 (24.4), 55 (87.0), 53 (24.9); (EI) HR-MS *m/z* $[M + H]^+$ 287.2011 (calcd for $C_{20}H_{31}O$, 287.2375).

***ent*-3*β*,18-Diacetoxy-19-trachylobanoic acid (12):** yellow solid; $[\alpha]_D^{20}$ −14.3 (*c* 8.03 $CHCl_3$); IR ν_{max} 2922, 2860, 1747, 1443, 1367, 1249, 1047 cm^{-1}; ^1H NMR Table 2; ^{13}C NMR Table 1; GC-MS *m/z* 359 (13.0), 358 (55.9), 343 (16.7) 302 (30.2), 287 (25.0), 283 (8.6), 239 (11.6), 183 (16.3), 169 (8.5), 159 (10.0), 147 (9.0), 145 (16.9), 143 (13.8), 133 (18.0), 132 (8.8), 131 (25.4), 129 (15.3), 121 (11.8), 120 (15.8), 119 (39.2), 118 (19.6), 117 (27.2), 114 (10.9), 107 (30.3), 106 (27.2), 104 (82.8), 103 (13.9), 93 (63.4), 91 (100.0), 81 (31.9), 80 (28.6), 79 (57.7), 78 (11.2), 77 (36.4), 67 (22.7), 65 (9.3), 61 (10.0), 55 (32.1), 53 (16.3).

***ent*-3*β*,18-Dihydroxytrachylobane (13):** white solid; $[\alpha]_D^{20}$ −24.0 (*c* 0.14 $CHCl_3$); IR ν_{max} 3423, 2926, 2855, 2358, 1730, 1443, 1383, 1043, 1005 cm^{-1}; ^1H NMR Table 2; ^{13}C NMR Table 1; GC-MS *m/z* $[M]^+$ 304 (7.0), 286 (7.0), 256 (9.3), 255 (34.9), 273, 248 (12.8), 201 (9.3), 199 (15.1), 185 (9.3), 176 (8.1), 175 (47.7), 173 (16.3), 161 (13.0), 159 (22.1), 157 (11.6), 147 (16.3), 145 (25.6), 143 (9.3), 135 (11.6), 133 (25.6), 132 (12.8), 131 (27.9), 121 (44.2), 120 (11.6), 119 (48.8), 118 (22.1), 117 (17.4), 109 (20.9), 108 (9.3), 107 (53.5), 105 (100.0), 95 (34.9), 93 (62.8), 92 (16.3), 91 (65.1), 81 (48.8), 79 (51.2), 77 (27.9), 69 (14.0), 67 (18.6), 57 (12.8), 55 (44.2), 53, (11.2); (EI) HR-MS *m/z* 304.2404 (calcd for $C_{20}H_{32}O_2$, 304.2404).

***ent*-3*β*-Hydroxy-17-trachylobanoic acid (14):** white gum; $[\alpha]_D^{20}$ −35.2 (*c* 0.29 $CHCl_3$); IR ν_{max} 3427, 2932, 2864, 1678, 1442, 1257, 1103, 1039, 1002 cm^{-1}; ^1H NMR Table 2; ^{13}C NMR Table 1; (EI) HR MS *m/z* 318.2192 (calcd for $C_{20}H_{30}O_3$, 318.2195).

Antimycobacterial Assay. The in vitro cell-based MABA anti-TB bioassay[20,22] was employed, using the virulent $H_{37}Rv$ strain of *M. tuberculosis* (ATCC 27294, American Type Culture Collection, Rockville, MD). Briefly, the test materials were incubated for 7−10 days with the mycobacteria in a 96-well-based microdilution format, and cell growth was determined using the Alamar Blue dye with fluorometric detection. MIC_{90} and percent inhibition values were calculated with reference to 1:10 dilutions of the inoculum. The MABA assay was chosen due to its versatility of capturing a wide array of anti-TB mechanisms of action, small sample requirements, low costs, and high-throughput capabilities; the MABA assay has been validated against the BACTEC clinical standard in anti-TB drug susceptibility testing.[20] Rifampin was used as a positive control, exhibiting an MIC of <0.12 mg/mL (<0.15 nmol/mL), while DMSO acted as a negative control.

Acknowledgment. A.S. and G.F.P. gratefully acknowledge support from FWF, Vienna, Austria, through a Schroedinger Postdoctoral Fellowship J2568 to A.S. The authors also thank Dr. R. Graf for help with the acquisition of MS spectra and Prof. Dr. R. Mues, Saarbrücken, Universität des Saarlandes, for his support in collecting and identifying the plant material. We are grateful to Mr. M. Niemitz, Perch Solutions, Kuopio, for his helpful and insightful NMR discussions. Finally we want to thank Dr. Des Callaghan for granting permission to use his photograph of *J. exsertifolia* in the TOC graphic.

Supporting Information Available: The ^1H and ^{13}C NMR spectra of the new compounds of this publication are available free of charge via the Internet at http://pubs.acs.org.

References and Notes

(1) WHO Global Tuberculosis Control Surveillance, Planning, Financing: WHO Report 2007; World Health Organization, 2007.
(2) Gale, G. A.; Kirtikara, K.; Pittayakhajonwut, P.; Sivichai, S.; Thebtaranonth, Y.; Thongpanchang, C.; Vichai, V. *Pharmacol. Ther.* **2007**, *115*, 307–351.
(3) Gibbons, S. *Phytochem. Rev.* **2005**, *4*, 63–78.
(4) Inui, T.; Wang, Y.; Deng, S.; Smith, D.; Franzblau, S.; Pauli, G. F. *J. Chromatogr. A* **2007**, *1151*, 211–215.
(5) Mitscher, L. A.; Rao, G. S. R.; Veysoglu, T.; Drake, S.; Haas, T. *J. Nat. Prod.* **1983**, *46*, 745–746.
(6) Asakawa, Y. *Phytochemisry of Bryophytes: Biologically Active Terpenoids and Aromatic Compounds from Liverworts*; Kluwer Academic/Plenum Publisher: New York, 1999.
(7) Abad, A.; Agulló, C.; Cuñat, A. C.; de Alfonso Marzal, I.; Navarro, I.; Gris, A. *Tetrahedron* **2006**, *62*, 3266–3283.
(8) Hugel, G.; Lods, L.; Mellor, J. M.; Theobald, D. W.; Ourisson, G. *Bull. Soc. Chim. Fr.* **1965**, *28*, 2882–2887.
(9) Harrison, L. J.; Asakawa, Y. *Phytochemistry* **1989**, *28*, 1533–1534.
(10) Fraga, B. M. *Phytochem. Anal.* **1994**, *5*, 49–56.
(11) Elliger, C. A.; Zinkel, D. F.; Chan, B. G.; Waiss, A. C. *Experentia* **1976**, *32*, 1364–1366.
(12) Mullin, C. A.; Alfatafta, A. A.; Harman, J. L.; Everett, S. L.; Serino, A. A. *J. Agric. Food Chem.* **1991**, *39*, 2293–2299.
(13) Block, S.; Baccelli, C.; Tinant, B.; Van Meervelt, L.; Rozenberg, R.; Habib Jiwan, J. L.; Llabres, G.; De Pauw-Gillet, M. C.; Quetin-Leclercq, J. *Phytochemistry* **2004**, *65*, 1165–1171.
(14) Zgoda-Pols, J. R.; Freyer, A. J.; Killmer, L. B.; Porter, J. R. *Fitoterapia* **2002**, *73*, 434–438.
(15) Trennheuser, M. L. *Phytochemische Untersuchung des Lebermooses Jungermannia exsertifolia*; Universität des Saarlandes: Saarbrücken (Germany), 1997.
(16) Block, S.; Stevigny, C.; De Pauw-Gillet, M. C.; De Hoffmann, E.; Llabres, G.; Adjakidje, V.; Quetin-Leclercq, J. *Planta Med.* **2002**, *68*, 647–649.
(17) Moraes, M.; Roque, N. F. *Phytochemistry* **1988**, *27*, 3205–3208.
(18) Garnot, O.; Amirav, A. In *Advances in LC MS Instrumentation*; Cappiello, A., Ed.; Elsevier, 2007; p 46.
(19) Kolehmainen, E.; Laihia, K.; Laatikainen, R.; Vepsalainen, J.; Niemitz, M.; Suontamo, R. *Magn. Reson. Chem.* **1997**, *35*, 463–467.
(20) Collins, L.; Franzblau, S. *Antimicrob. Agents Chemother.* **1997**, *41*, 1004–1009.
(21) Adam, K. P.; Thiel, R.; Zapp, J.; Becker, H. *Arch. Biochem. Biophys.* **1998**, *354*, 181–187.
(22) Franzblau, S. G.; Witzig, R. S.; McLaughlin, J. C.; Torres, P.; Madico, G.; Hernandez, A.; Degnan, M. T.; Cook, M. B.; Quenzer, V. K.; Ferguson, R. M.; Gilman, R. H. *J. Clin. Microbiol.* **1998**, *36*, 362–366.
(23) Niemitz, M.; Laatikainen, R.; Chen, S. N.; Kleps, R.; Kozikowski, A. P.; Pauli, G. F. *Magn. Reson. Chem.* **2007**, *45*, 878–882.
(24) Ngouela, S.; Nyassé, B.; Tsamo, E.; Brochier, M.-C.; Morin, C. *J. Nat. Prod.* **1998**, *61*, 264–266.

NP900806J